

Bacterial Photodynamic Inactivation Mediated by Methylene Blue and Red Light Is Enhanced by Synergistic Effect of Potassium Iodide

Daniela Vecchio,^{a,b} Asheesh Gupta,^{a,b,c} Liyi Huang,^{a,b,d} Giacomo Landi,^{a,e} Pinar Avci,^{a,b,f} Andrea Rodas,^{a,b,g}
Michael R. Hamblin^{a,b,h}

Wellman Center for Photomedicine, Massachusetts General Hospital, Boston, Massachusetts, USA^a; Department of Dermatology, Harvard Medical School, Boston, Massachusetts, USA^b; Defence Institute of Physiology and Allied Sciences (DIPAS), Delhi, India^c; Department of Infectious Diseases, First Affiliated College and Hospital, Guangxi Medical University, Nanning, China^d; Department of Molecular Medicine, University of Siena, Siena, Italy^e; Department of Dermatology, Dermatocology and Venerology, Semmelweis University School of Medicine, Budapest, Hungary^f; Center for Lasers and Applications, Nuclear and Energy Research Institute, Sao Paulo, Brazil^g; Harvard-MIT Division of Health Sciences and Technology, Cambridge, Massachusetts, USA^h

The inexorable increase of antibiotic resistance occurring in different bacterial species is increasing the interest in developing new antimicrobial treatments that will be equally effective against multidrug-resistant strains and will not themselves induce resistance. One of these alternatives may be photodynamic inactivation (PDI), which uses a combination of nontoxic dyes, called photosensitizers (PS), excited by harmless visible light to generate reactive oxygen species (ROS) by type 1 (radical) and type 2 (singlet oxygen) pathways. In this study, we asked whether it was possible to improve the efficacy of PDI *in vitro* and *in vivo* by addition of the inert salt potassium iodide (KI) to a commonly investigated PS, the phenothiazinium dye methylene blue (MB). By adding KI, we observed a consistent increase of red light-mediated bacterial killing of Gram-positive and Gram-negative species *in vitro* and *in vivo*. *In vivo*, we also observed less bacterial recurrence in wounds in the days posttreatment. The mechanism of action is probably due to formation of reactive iodine species that are produced quickly with a short lifetime. This finding may have a relevant clinical impact by reducing the risk of amputation and, in some cases, the risk of death, leading to improvement in the care of patients affected by localized infections.

The ever-growing spread of antibiotic resistance has given new urgency to the search for antimicrobial methodologies to which microbes are thought to be unable to develop resistance (1). Photodynamic inactivation (PDI) is an alternative approach to kill multidrug-resistant microorganisms using a combination of nontoxic dyes and harmless visible light. PDI employs a nontoxic dye called a photosensitizer (PS) together with low-intensity visible light. In the presence of oxygen, light induces the formation of reactive oxidative species (ROS). These ROS are generated by energy or electron transfer from the PS long-lived triplet excited state that is able to oxidize biomolecules and thereby kill cells (2).

The photochemistry from the PS triplet state can occur by two parallel pathways. Type 1 involves electron transfer to oxygen initially forming superoxide and eventually producing cytotoxic hydroxyl radicals, while type 2 involves energy transfer to ground-state triplet oxygen and production of cytotoxic singlet oxygen. It is known that the selectivity of the PS for bacteria over host tissue can be obtained by the appropriate chemical design to ensure that the molecule will preferentially bind to bacterial cells rather than mammalian cells particularly at short incubation times (3–5).

Although many advances in the chemical design of new PSs have been made, there are still limitations in PDI and recurrence of bacterial growth may occur in animal studies after completion of the illumination.

Many researchers use methylene blue (MB), a phenothiazinium dye, which is the most commonly studied antimicrobial PS in the literature. Several studies have reported its activity *in vitro* and in animal models of infection, and MB has received regulatory approval to mediate photodynamic therapy (PDT) of dental infectious diseases (6–8), such as periodontitis and caries (9, 10), and is under clinical investigation for nasal decontamination and chronic sinusitis in some countries.

MB is well known to act by the type 1 mechanism (producing reactive oxygen species including hydroxyl radicals) and also by the type 2 mechanism (producing singlet oxygen); however, singlet oxygen is more often credited with being the most effective antimicrobial species produced during PDT.

We recently observed a consistent improvement of PDT efficacy *in vitro* against Gram-positive *Staphylococcus aureus* and Gram-negative *Escherichia coli* because of the addition of sodium azide (11) or sodium thiocyanate (12) to the MB solution used for PDI. Even though this discovery is interesting because of the photochemistry, and to clarify the mechanisms and the species involved in the enhancement of bacterial killing, these compounds unfortunately cannot be used in clinical applications due to their toxicity. For this reason, our interest in the present study moved on to investigate the effect of the inert inorganic salt potassium iodide (KI) in combination with PDI using MB. The safe and effective use of KI was reported in 2001 in a Food and Drug Administration (FDA) document (13). Moreover, KI is contained at a certain percentage in Lugol's solution used as an antiseptic and

Received 5 January 2015 Returned for modification 28 January 2015

Accepted 6 June 2015

Accepted manuscript posted online 15 June 2015

Citation Vecchio D, Gupta A, Huang L, Landi G, Avci P, Rodas A, Hamblin MR. 2015. Bacterial photodynamic inactivation mediated by methylene blue and red light is enhanced by synergistic effect of potassium iodide. *Antimicrob Agents Chemother* 59:5203–5212. doi:10.1128/AAC.00019-15.

Address correspondence to Michael R. Hamblin, hamblin@helix.mgh.harvard.edu.

Copyright © 2015, American Society for Microbiology. All Rights Reserved.

doi:10.1128/AAC.00019-15

disinfectant. It is applied for several applications, and its side effects are well known (14–16).

In the present paper, we asked whether the synergistic effect of PDI in combination with KI can increase bacterial killing *in vitro* and *in vivo*. Bacterial killing was tested *in vitro* against *S. aureus* and *E. coli* using different concentrations of MB with a constant concentration of KI and also with the converse. We also demonstrated the PDI effect by testing a range of different light doses, and we clarified some mechanisms that might explain the enhancement of killing observed in our study.

Finally, we used an *in vivo* model of localized infection consisting of mouse burn wounds. Burn wounds are clinically relevant since they are relatively common and they can easily become infected.

MATERIALS AND METHODS

***In vitro* study.** (i) **Chemicals and reagents.** Methylene blue (MB), potassium iodide (KI), Lugol's solution, and all other reagents were purchased from Sigma-Aldrich (St. Louis, MO) unless otherwise indicated. MB stock solution was prepared in distilled H₂O (dH₂O) and stored at 4°C in the dark for no more than 24 h prior to use. KI solution was prepared in dH₂O as required immediately before experimentation. The singlet oxygen sensor green (SOSG) and hydroxyphenyl fluorescein (HPF) probes to detect singlet oxygen or hydroxyl radicals were purchased from Life Technologies (Grand Island, NY, USA).

(ii) **Bacterial strains and culture conditions.** *Staphylococcus aureus* (NCTC 8325) and *Escherichia coli* K-12 (ATCC 33780) were chosen as representative Gram-positive and Gram-negative bacteria, respectively, for *in vitro* studies. A colony of bacteria was suspended in 25 ml of brain heart infusion (BHI) broth (Becton, Dickinson, and Company, Franklin Lakes, NJ) and grown overnight in a shaker incubator (New Brunswick Scientific, Edison, NJ) at 120 rpm under aerobic conditions at 37°C. An aliquot of 1 ml from an overnight suspension was refreshed in fresh BHI for 2 h at 37°C to mid-log phase. Cell concentration was estimated by measuring the optical density (OD) at 600 nm (OD of 0.8 = 10⁸ CFU cells/ml). The bacterial suspension was centrifuged, washed, and resuspended in phosphate-buffered saline (PBS) to arrest microbial growth and used (10⁸ CFU) for the *in vitro* or *in vivo* experiments.

(iii) **Potential of MB-antibacterial PDI by addition of potassium iodide *in vitro*.** In order to test if the addition of KI can increase the MB-mediated PDI bacteria inactivation, we performed different experiments. These experiments also revealed the parameters that are relevant in increasing bacteria inactivation. First, we carried out PDI *in vitro* studies with *S. aureus* and with *E. coli*. Cells (10⁸ CFU; 500 μl) were incubated with different concentrations of MB (0 to 50 μM) for 15 min with or without the addition of 10 mM KI. An aliquot of 100 μl was used as the dark control (DC) from each sample; another aliquot (100 μl) was irradiated with a 5-J/cm² dose of light (660 nm light) and then placed in a new 96-well plate. The aliquots were serially diluted 10-fold in PBS to give dilutions of 10¹ to 10⁵ times in addition to the original concentration. From each dilution, 10-μl aliquots were seeded horizontally on BHI agar. Plates were streaked in triplicate and incubated for 14 to 18 h at 37°C in the dark to allow the growth of colonies. Each experiment was performed at least three times.

To verify if the bacterial inactivation was also dependent on the light dose, we treated the cells with a single concentration of MB (10 μM) and KI (10 mM), and we irradiated with a range of doses of light (0 to 7 J/cm²). After treatment, an aliquot from each group of treatment was placed in a new 96-well plate, and serial dilution was performed as described above.

Finally, to investigate the dependency of bacteria inactivation by KI concentration, we performed the same experiment using 10 μM MB and 5 J/cm² of red light and added a range of KI concentrations between 0 and 10 mM just before delivering the light.

(iv) **Potassium iodide toxicity on bacterial cells.** We carried out *in vitro* cytotoxicity studies with *S. aureus* and *E. coli*. The cells (10⁸ CFU; 500 μl) were incubated with different concentrations of KI (0 to 50 mM) for 10 min in order to verify the toxicity of KI. An aliquot of 100 μl from each sample was used as the dark control, and another aliquot (100 μl) was irradiated with a 5-J/cm² dose of light (660 nm light) and then placed in a new 96-well plate. The aliquots were serially diluted as before.

(v) **Potassium iodide toxicity on human dermal skin fibroblast and culture conditions.** Human dermal fibroblasts (HDF) were a generous gift from Tsao Lab (Wellman Center for Photomedicine, Boston, MA, USA). The cells were cultured in Dulbecco modified Eagle medium (DMEM) with L-glutamine and NaHCO₃ supplemented with 10% heat-inactivated fetal bovine serum, penicillin (100 U/ml), and streptomycin (100 μg/ml) (Sigma, St. Louis, MO) at 37°C in 5% CO₂ humidified atmosphere in 75 cm² flasks (Falcon; Invitrogen, Carlsbad, CA). When HDF cells reached 80% confluence, they were washed with PBS and harvested with 2.0 ml of 0.25% trypsin-EDTA solution (Sigma). Cells were then centrifuged and counted in trypan blue to ensure viability and plated in white/clear flat-bottom 96-well plates (BD Falcon). Cells were allowed to attach overnight. When the cells reached around 80% confluence, dilutions of the KI were prepared in complete phenol red-free DMEM (31053-028; Gibco Life Technologies), and cell culture medium was replaced with KI at final concentrations of 10, 20, 30, 40, and 50 mM. Following incubation with KI for 20 min, the cells were either irradiated or not with a 5-J/cm² dose of light at a 660-nm wavelength. After treatment, the cells were washed with PBS, replaced with fresh complete medium, and incubated overnight. The cellular viability was determined by PrestoBlue assay (PrestoBlue cell viability reagent; Invitrogen). Briefly, 10 μl PrestoBlue solution was added to each well and incubated for 90 min at 37°C. Then, the fluorescence was determined at 560-nm excitation and 590-nm emission by a microplate spectrophotometer (SpectraMax 340PC). For each sample, the cellular viability was calculated from the data of 3 wells (*n* = 3) and expressed as a percentage, compared with the untreated cells (100%). Comparison of the mean optical density between the untreated (100%) and treated cells with KI allowed the evaluation of the cytotoxicity. Each experiment was repeated 3 times.

(vi) **ROS probe study.** Fluorescent probe experiments were performed in 96-well black-sided plates. A final concentration of 10 μM SOSG or HPF was added to 5 μM MB solution with or without the addition of KI in 100 μl PBS per well. Fluorescence spectrometry (SpectraMax M5 plate reader; Molecular Devices, Sunnyvale, CA) used excitation and emission at 504 and 525 nm for SOSG and 490 and 515 nm for HPF, respectively. A range of light doses (0 to 10 J/cm²) was delivered using red light (660 ± 15 nm band-pass filter) at an irradiance of 100 mW/cm² as measured with a power meter (model DMM 199 with 201 standard head; Coherent, Santa Clara, CA). The fluorescence was measured after each dose of light was delivered.

(vii) **Iodine generation.** UV-visible (UV-Vis) spectral analysis was carried out using UV-Vis spectra monitored in a solution containing 10 μM MB and 10 mM KI buffered with PBS, and spectra were measured before and after shining 5 J/cm² of light. As a reference, spectra were obtained from a 1:160 dilution of Lugol's solution in PBS.

To verify whether the generation of I₂ was responsible for killing the bacteria, we irradiated (with 7 J/cm² light) a solution of MB (10 μM) with and without addition of 10 mM KI, and then we added 10⁸ CFU bacterial cells to the treated solutions for the range of 0 to 30 min. CFU were measured as already described.

(viii) **Fenton and H₂O₂ plus HRP reactions.** Suspensions of bacteria (10⁸ CFU/ml) were incubated at room temperature with various concentrations of Fenton reagent (equal concentrations of H₂O₂ and FeSO₄) or with 10 mM H₂O₂ plus HRP (0 to 8 IU) with or without the addition of 10 mM KI. In the two experiments, bacterial cells were incubated with reagents diluted in pH 7.4 PBS for 1 h. At the end of the incubation time, 100-μl aliquots were placed in 96 wells from each tube and serially diluted on agar plates to determine CFU.

In vivo study. (i) Bacterial strain and culture conditions. The *S. aureus* strain used in this work was USA300 LAC (Los Angeles County clone), a community-acquired methicillin-resistant *S. aureus* (CA-MRSA) strain. USA300 LAC was chromosomally transduced with the transposon for the bacterial luciferase gene operon *lux* ABCDE (pAUL-ATn4001 lx ABCDE Km; Caliper Life Sciences, Hopkinton, MA) to give USA300 LAC:*lux*, allowing real-time monitoring of the extent of bacterial infection in living mice (17). Bacteria were routinely grown in brain heart infusion (BHI) broth (Fischer Scientific) with aeration in an orbital incubator at 100 rpm at 37°C overnight to stationary phase. An aliquot of this suspension was then refreshed in fresh BHI to mid-log phase. Cell numbers were estimated by measuring the optical density (OD) at 600 nm (OD of 0.8 = 10⁸ CFU cells/ml). Bacterial suspension was centrifuged, washed, and resuspended in PBS and used for the *in vivo* experiments.

(ii) MRSA (USA300) burn infection in mice. All animal procedures were approved by the IACUC of the Massachusetts General Hospital (2005N000096) and were in accordance with the guidelines of the National Institutes of Health (NIH). Adult 7- to 8-week-old female BALB/c mice weighing 17 to 21 g were obtained from Charles River Laboratories (Wilmington, MA). The animals were housed one per cage with *ad libitum* access to food and water and were maintained on a 12-hour light-dark cycle at a room temperature of around 21°C and a relative humidity range of 30 to 70%. Before the creation of burns, the mice were anesthetized by intraperitoneal (i.p.) injection of a ketamine-xylazine cocktail and shaved on the dorsal surface. Burns were incurred by applying a preheated (~95°C) brass block to the dorsal surface of each mouse for 3 s, resulting in nonlethal full-thickness third-degree burns measuring approximately 1.2 cm by 1.2 cm. Five minutes after incurrence of the burn, a 60- μ l bacterial suspension containing 10⁸ CFU of bioluminescent MRSA in PBS was inoculated and then smeared onto the burn wound surface with an inoculating loop. Bioluminescence images were taken just after the inoculation of bacteria and 30 min after inoculation.

(iii) Photodynamic therapy. Thirty mice were randomly divided into five groups of six animals each; these groups were designated as follows: PDT treated with mixture of MB (50 μ M) plus KI (10 mM) and 660 nm light (A), PDT treated with MB (50 μ M) alone (B), light-alone control (C), dark control treated with mixture of MB plus KI but without light illumination (D), and infected burn control that received no treatment (E). Thirty minutes after the infection, a solution of 30 μ l MB plus KI or MB alone was added to groups, 15 minutes was allowed for PS to bind to and penetrate the bacteria, and mice were again imaged to quantify any dark toxicity.

(iv) Bioluminescence imaging. The setup consisted of an intensified charge-coupled device (ICCD) camera (model C2400-30H; Hamamatsu Photonics, Bridgewater, NJ), a camera controller, an imaging box, an image processor (C5510-50; Hamamatsu), and a color monitor (PVM 1454Q; Hamamatsu). Light-emitting diodes were mounted inside the imaging box to supply the light required for obtaining dimensional imaging of the sample. Under the photocounting mode, a clear image can be obtained even at extremely low light levels by detecting and integrating individual photons one by one. Prior to imaging, the mice were anesthetized by i.p. injections of a ketamine-xylazine cocktail. The mice were then placed on an adjustable stage in the specimen chamber, and the infected burns were positioned directly under the camera. A grayscale background image of each wound was made, and this was followed by a photon count of the same region. This entire burn photon count was quantified as relative luminescence units (RLUs) and was displayed in a false-color scale ranging from pink (most intense) to blue (least intense). Red light (660 \pm 15 nm) was initiated at 30 min after bacterial inoculation and 15 min later followed by PS application with an irradiance of 100 mW/cm². The mice were given a total light exposure of up to 150 J/cm² in aliquots with bioluminescence imaging taking place after each aliquot of light. To record the time course of the extent of bacterial infection, the bacterial bioluminescence from mouse burns was measured daily after PDT until

the infections were cured (characterized by the disappearance of bacterial luminescence) or the burns were healed.

(v) Statistical analyses. Statistical analyses were performed for PDI studies. One-way analysis of variance (ANOVA) and the Tukey *post hoc* test were used to compare survival fractions of PDT plus KI with PDT alone. Analysis was performed using Microsoft Excel Statistical Package (Microsoft, Redmond, Washington). Results were considered statistically significant with a *P* of <0.05.

RESULTS AND DISCUSSION

Bacterial resistance to antibiotics is one of the most serious health threats facing the world today (1). For this reason, there is some urgency to the search for new nonantibiotic antimicrobial treatments. Several studies reported in the literature have demonstrated the ability of PDI to kill a wide range of microorganisms *in vitro* and have further shown that PDT can effectively treat animal models of localized infections.

However, the recurrence of bacteria in the infection can occur once the bactericidal effect of the light/PS combination ceases. The innovation offered by adding KI to the PS solution is that by interaction of the ROS and KI during light exposure, biocidal molecular iodine (I₂ and/or I₃⁻) or hypoiodous acid (HOI) can be generated, thereby improving bacterial killing. Alternatively, reactive iodide radicals (I[•] or I₂^{•-}) may be formed by interaction of the PS excited state (or hydroxyl radicals) with KI that would increase the damage to bacterial cell wall constituents. The increase in PDI efficacy may have a relevant clinical impact on eradication of infection. Our hypothesis was that the synergistic activity of KI (a harmless and inert salt) and photoexcited MB can increase the therapeutic efficacy compared to PDT alone *in vitro* and *in vivo* studies. Moreover, we wanted to clarify the potential mechanism of action that may determine the enhancement of bacterial killing.

Potential of MB-antibacterial PDI by addition of potassium iodide *in vitro*. Results in Fig. 1 show the survival fraction curves obtained against the Gram-positive bacterium *S. aureus* (Fig. 1A) or Gram-negative bacterium *E. coli* (Fig. 1B) incubated for 20 min with a range of 0 to 100 μ M MB concentrations for strains with and without addition of 10 mM KI. The addition of KI produced increases in bacterial killing of 4 and 2 logs for *S. aureus* and *E. coli*, respectively.

Moreover, to verify the light-dependent photochemical process in the bacterial killing, we also show the survival fraction curves obtained against *S. aureus* (Fig. 1C) or *E. coli* (Fig. 1D) incubated for 20 min with 10 μ M MB for the two strains with and without 10 mM KI and delivering increasing doses of light (0 to 7 J/cm²). In these experiments, when we added KI, we observed an increase in bacterial killing for the two strains. The increased killing in each of the experiments was more pronounced in *S. aureus* than *E. coli*.

We also studied the bacterial killing after adding different concentrations of KI (0 to 10 mM) to *S. aureus* (Fig. 1E) and *E. coli* (Fig. 1F). The results showed a dose-dependent increase of bacterial killing in *S. aureus* starting from 0.01 mM KI while the enhancement of *E. coli* killing was only observed with 5 mM KI.

A key parameter in PDI was also investigated. The binding of PS to the cell membrane or the uptake of PS into the cells obtained during incubation with MB is a critical point in PDI. For this reason, we verified the bacterial killing in the presence or not of KI with and without washing the cells with PBS after MB incubation and before adding KI to *S. aureus* and *E. coli* (data not shown).

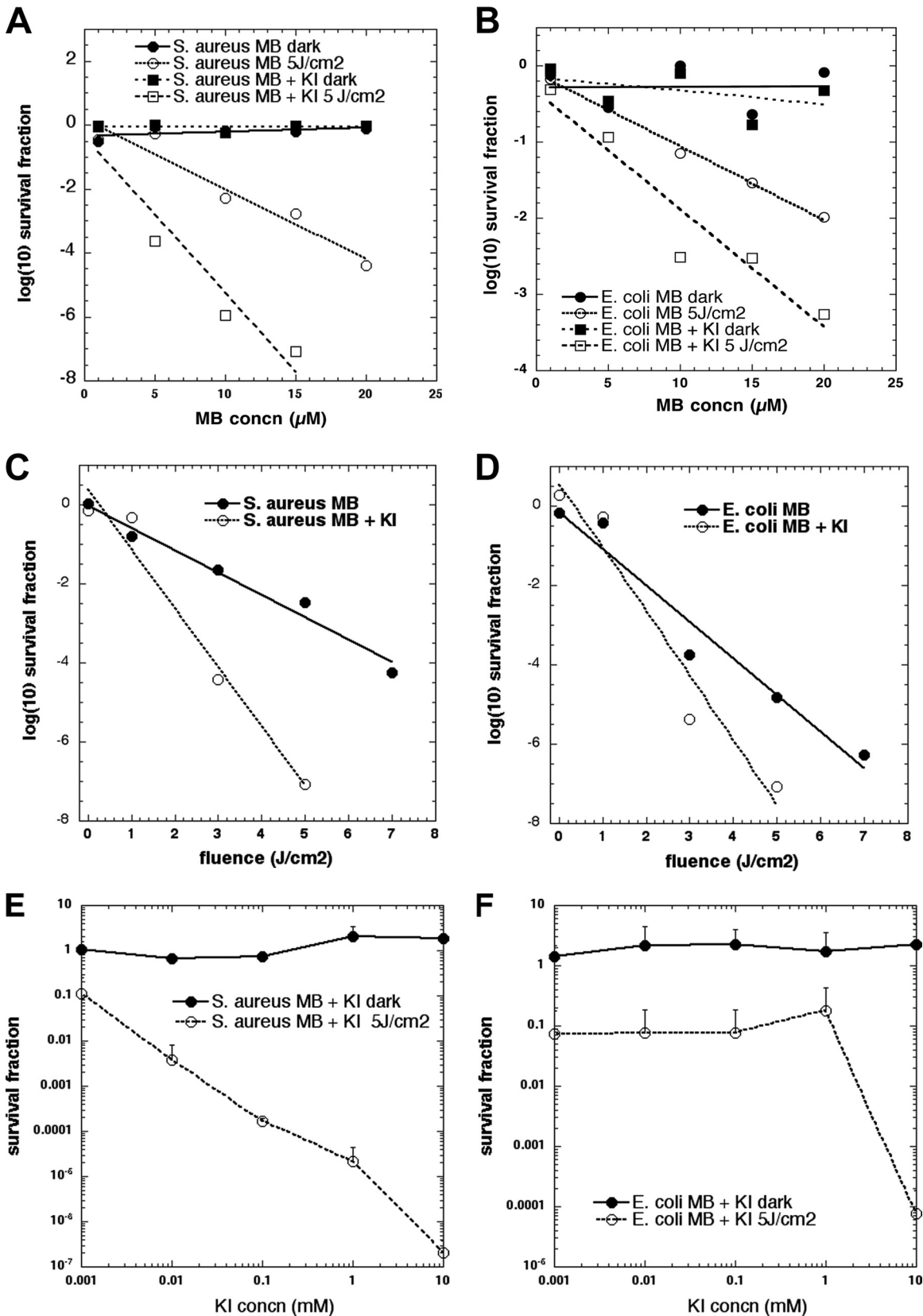


FIG 1 Effect of KI on MB-mediated PDT of bacteria. *S. aureus* (A) or *E. coli* (B) bacteria (10^8 cells/ml) were incubated with a range of MB concentrations for 15 min followed or not by addition of KI and illumination with 5 J/cm^2 of a 660-nm light. *S. aureus* (C) or *E. coli* (D) bacteria (10^8 cells/ml) were incubated with an MB concentration of $10 \mu\text{M}$ for 15 min followed by addition of KI (10 mM) and illumination with different fluences (0 to 7 J/cm^2) of 660-nm light. (E and F) Different concentrations of KI (0.01 to 10 mM) were tested with MB-PDT against bacteria. (A to D) Best linear fit curves. *S. aureus* (E) or *E. coli* (F) bacteria (10^8 cells/ml) were incubated with $10 \mu\text{M}$ MB followed by addition of a range of KI concentrations and illumination with 5 J/cm^2 of 660-nm light.

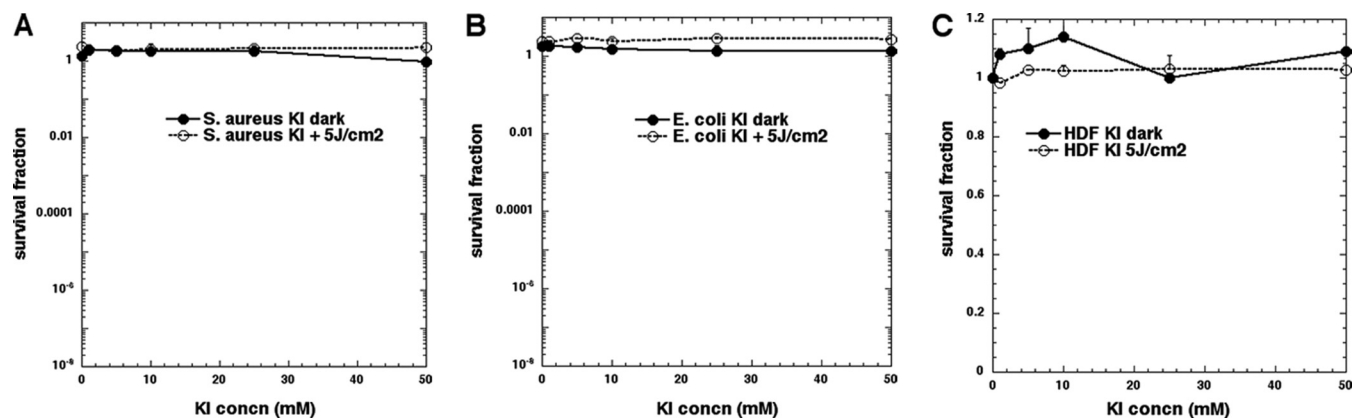


FIG 2 Effect of KI on *S. aureus* (A), *E. coli* (B), and human dermal skin fibroblasts (C). (A, B) Bacterial cells (10^8 CFU, $500 \mu\text{l}$) were incubated with different concentrations of KI (0 to 50 mM) for 10 min in order to verify the toxicity of KI followed or not by irradiation with $5 \text{ J}/\text{cm}^2$ of a 660-nm light. Human dermal skin fibroblasts (C), upon reaching 80% confluence, were incubated with KI (10 to 50 mM) for 20 min followed by illumination or not with $5 \text{ J}/\text{cm}^2$ of a 660-nm light. Cell viability was evaluated by PrestoBlue assay.

Cells were then either exposed (light) or not (dark) to a range of light doses 0 to $5 \text{ J}/\text{cm}^2$ at an irradiance of $100 \text{ mW}/\text{cm}^2$. For the dark control (DC), we incorporated the time of light exposure. Cells were then serially diluted and plated to count CFU. Survival fractions showed that an enhancement of bacterial killing in the presence of KI was observed in the two strains without a wash while no killing was observed after washing of the MB solution from the cells. The presence of unbound MB in the solution is therefore critical under our experimental conditions.

The lack of killing without light under all experimental conditions showed that neither the MB alone nor MB plus KI displayed any appreciable dark toxicity. On the basis of these results, we concluded that the presence of KI can increase bacterial killing depending on the doses of MB and light and on the KI concentration. Moreover, the binding of MB to the cell membrane is not involved in the increase in bacterial PDI.

Effect of potassium iodide alone on bacteria and mammalian cells *in vitro*. Since it is well known in the literature that KI itself

can exert an antimicrobial effect, we tested a larger range of KI concentrations (0 to 50 mM) on bacterial (Fig. 2A and B) and mammalian cells (Fig. 2C) to verify that KI itself was not responsible for the effect observed in our experiments. Our results (Fig. 2) show that after a 10-min incubation of *S. aureus* (Fig. 2A) or *E. coli* (Fig. 2B), there was no bacterial killing either in dark controls or after shining a $5 \text{ J}/\text{cm}^2$ dose of light.

To ensure that KI does not have any side effect in *in vivo* experiments, we investigated the effect of KI *in vitro* on mammalian dermal skin fibroblasts. As shown in Fig. 2C, KI did not kill mammalian cells exposed for 20 min to the range of KI concentration (0 to 50 mM) either in dark controls or after shining a $5 \text{ J}/\text{cm}^2$ dose of light.

These results suggested that the observed potentiation of bacterial photokilling is due to the synergistic effect of MB-PDI and KI used together.

Fluorescence probe experiments. In order to clarify the mechanisms involved in the effect observed on bacterial killing, we used

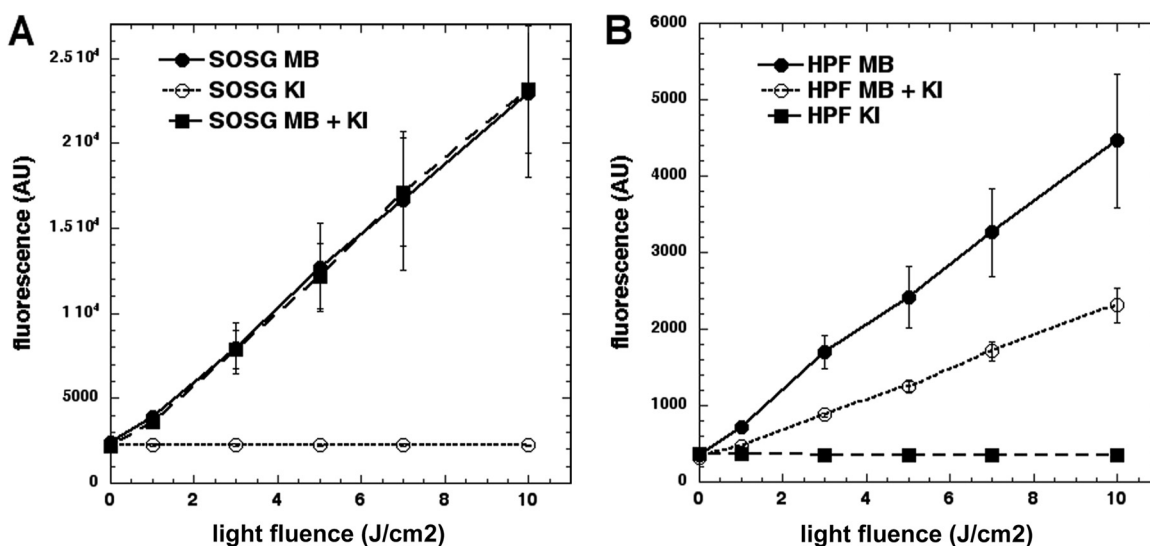


FIG 3 Fluorescence ROS probe studies with photoactivated MB in the presence or not of KI. Fluorescence generated from probes (SISG and HPF, $10 \mu\text{M}$) and MB ($5 \mu\text{M}$) in water without addition and with addition of 10 mM KI. (A) MB, KI, MB + KI, and SOSG, red light; (B) MB, KI, MB + KI, and HPF, red light.

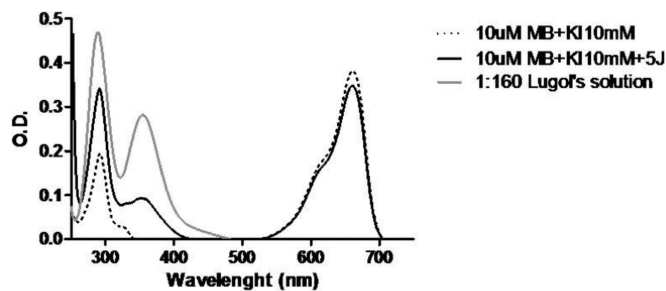


FIG 4 Iodine absorption spectra. The spectra of the solution containing 10 μM MB and 10 mM KI buffered with PBS were determined before and after irradiation with 5 J/cm^2 of light to verify the generation of iodine species. As a control, we used the spectrum obtained from the 1:160 dilution of Lugol's solution.

fluorescent probes, in particular, SOSG as a marker of singlet oxygen and HPF as a marker for hydroxyl radical generation. The presence of KI did not produce any difference in SOSG activation (Fig. 3A) while we observed a quenching phenomenon for HPF

(Fig. 3B). This quenching of HPF suggests that it is more likely that hydroxyl radicals receive an electron transfer from iodide, producing an iodide radical (and hydroxide anion), than it is that the excited MB receives an electron transfer from iodide (producing an iodide radical and MB radical).

It has been reported in the literature by Miyachi and Niwa (18) that KI decreased the *in vitro* generation of ROS produced by polymorphonuclear leukocytes (PMN). In particular, they showed that KI in a range of concentrations of 0.1 μM to 1 mM was able to decrease consistently the generation of hydrogen peroxide (H_2O_2) and hydroxyl radical (HO^\bullet) while giving no reduction of the superoxide anion (O_2^-). This may explain the reduction in probe activation observed in our system.

Iodine generation. To verify the generation of iodine in our system, we ran the spectra of MB and MB plus KI solutions before and after shining the light. The generation of iodine species was evaluated by measuring the peak at 348 nm (19). Our positive control was Lugol's solution diluted and combined with MB. As shown in Fig. 4, we observed the production of iodine species

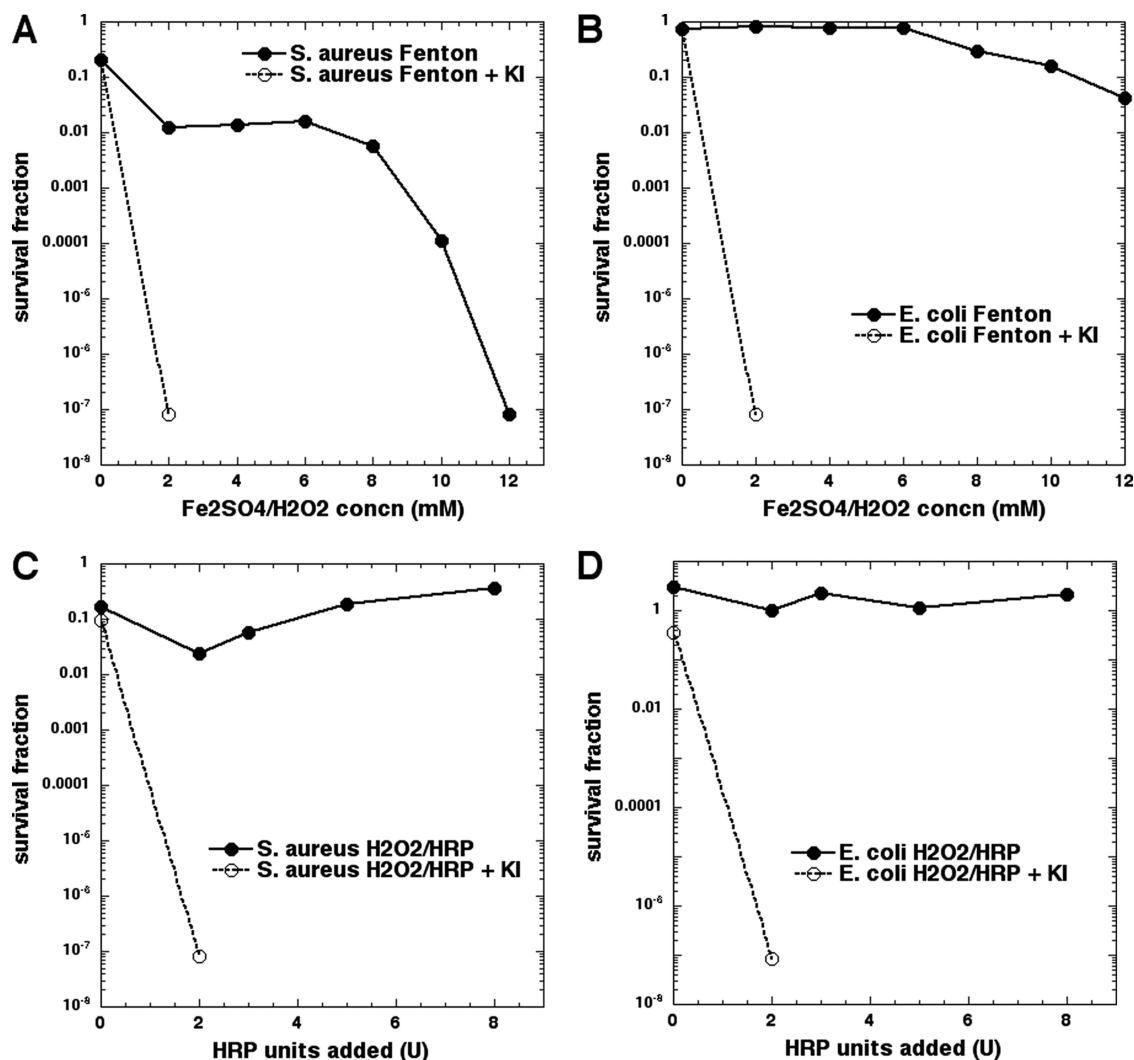


FIG 5 Effect of KI on Fenton reagent and H_2O_2 /HRP killing of bacteria. *S. aureus* (A) or *E. coli* (B) (10^8 cells/ml) was incubated with the stated equimolar concentrations of H_2O_2 and FeSO_4 with and without KI (10 mM) for 1 h. *S. aureus* (C) or *E. coli* (D) (10^8 cells/ml) bacteria were incubated with 10 mM H_2O_2 and different numbers of units (U) of HRP with and without KI (10 mM) for 1 h.

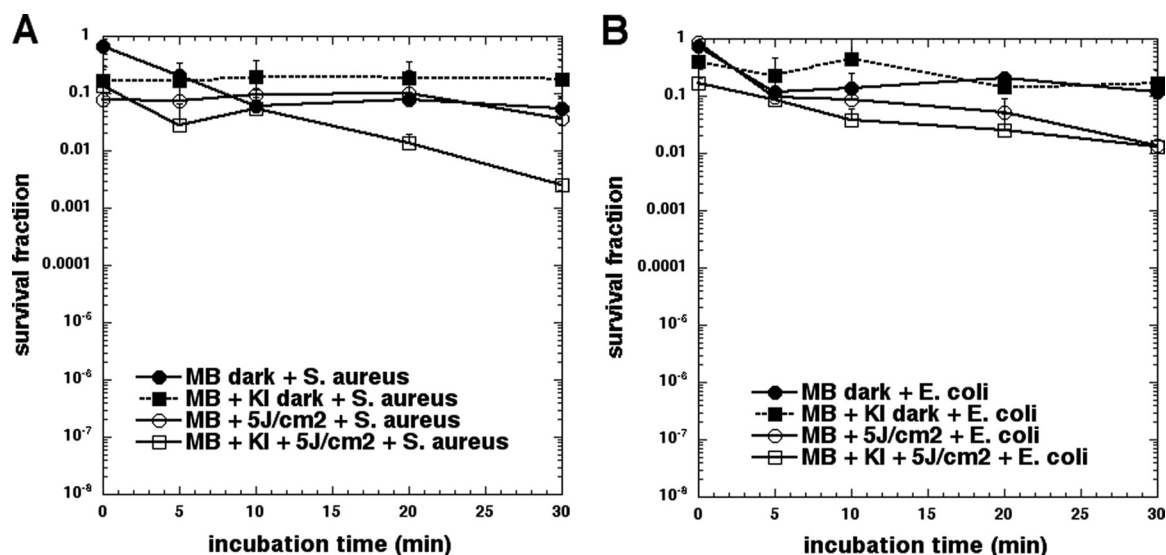


FIG 6 Can killing be explained by iodine generation? The solution of MB (10 μ M) with and without addition of 10 mM KI was irradiated with 7 J/cm² light followed by the addition of bacterial cells, *S. aureus* (A) and *E. coli* (B) (10^8 cells/ml). Bacteria killing was evaluated in the range of 0 to 30 min.

when we delivered 5 J/cm² while no peak was observed in the spectra before shining the light.

Effect of added KI to Fenton reagent or to a mixture of H₂O₂ and NaOCl to potentiate bacterial killing. The plots in Fig. 5 show the antimicrobial activity of the Fenton reagent (ratio of FeSO₄/H₂O₂ was 1:1) and of a combination (Fenton reagent plus KI) against *S. aureus* (Fig. 5A) and *E. coli* (Fig. 5B). When Fenton reagent was combined with 10 mM KI, we observed a dramatic potentiation (up to 6 logs) of the antimicrobial effect of the Fenton reaction. This may imply that HO[•] reacted with KI, producing iodide radicals from HO[•], which potentiated bacterial killing in cell suspension.

The addition of Iodide to the Fenton reaction to potentiate bacterial killing has been investigated in the past. Klebanoff (20) observed that when using the Fenton reaction in the presence of iodide, the bacterial killing was increased. They explained that the potentiation of bacterial killing involved the oxidation of iodide by hydroxyl radicals. Other studies demonstrated that iodide can potentiate the Fenton reagent killing of microorganisms such as *Aspergillus fumigatus* and *Candida albicans* (21) and also *Blastomyces dermatitidis* (22).

We observed the same dramatic potentiation in bacterial killing (about 6 logs) when we added KI to the reaction mixture of H₂O₂ plus horseradish peroxidase (HRP). It has again been reported in the literature (23, 24) that iodide can potentiate microbial killing by different kinds of peroxidase enzymes (myeloperoxidase, lactoperoxidase [LP], HRP) in combination with H₂O₂. The mechanism of action was proposed to be oxidation of iodide anion to iodine radicals by the enzyme-hydrogen peroxide transition state (25) (as originally worked out by Chance in 1943 [26]).

Does production of long-lived reactive iodine species (I₂, I₃⁻, or HOI) explain bacterial killing? To verify whether long-lived (relatively stable) species such as molecular iodine (I₂) or hypoiodous acid (HOI) are responsible for increased bacterial killing, we added bacteria after completion of light delivery.

We irradiated the solutions containing MB or MB plus KI with 5 J/cm² of 660 nm light to generate the iodine species observed in

the spectra described above. Molecular iodine is a stable molecule and even HOI is reasonably stable with a measurable half-life, so we asked whether by incubating the cells in a solution that can contain photochemically produced bactericidal concentrations of I₂ or HOI, we would observe bacterial killing after the light had been switched off. We added bacterial cells to the photoactivated MB plus KI solution, and we evaluated the survival fraction of bacteria after incubation times ranging between 5 and 30 min. As shown in the plots (Fig. 6), we did not observe any bacterial killing in either strain. This finding demonstrated that even if our system generated some I₂ and/or HOI, there was no evidence that the concentration produced can be responsible for the enhanced bacterial killing observed with MB-PDI in the presence of KI. No killing was observed in the dark control. The addition of KI to potentiate the lactoperoxidase (LP) plus hydrogen peroxide system (which is thought to produce HO[•] or equivalent) has been reported in the literature to decrease dental plaque formation (27). This system has also been used as a preservative in foods and pharmaceuticals by increasing the fungicidal and bactericidal effect against *Candida albicans*, *E. coli*, and *S. aureus* (28).

In vivo studies in a murine burn infection model using bioluminescent MRSA and in vivo imaging. Since the results obtained *in vitro* showed an impressive potentiation of bacterial killing, we wanted to verify that it was possible to increase the efficacy of PDT-mediated bacterial killing by adding KI to MB in an *in vivo* infection model.

The infected burn was treated with 50 μ M MB, with and without the addition of 10 mM KI, and excited with 660 nm light at up to 150 J/cm², while the control groups were dark controls with the same amount of MB plus KI and the light-alone control received 660 nm light to 150 J/cm². Figure 7 shows a set of five representative bioluminescence image time courses from burns (each time course from a single mouse in each of the 5 groups) infected with MRSA. The bacterial bioluminescence was largely preserved in the infected burn control (Fig. 7E) during the treatment with light alone (Fig. 7C) and in dark controls of MB plus KI (Fig. 7D). In contrast, PDT gave a light dose-dependent reduction of bacterial

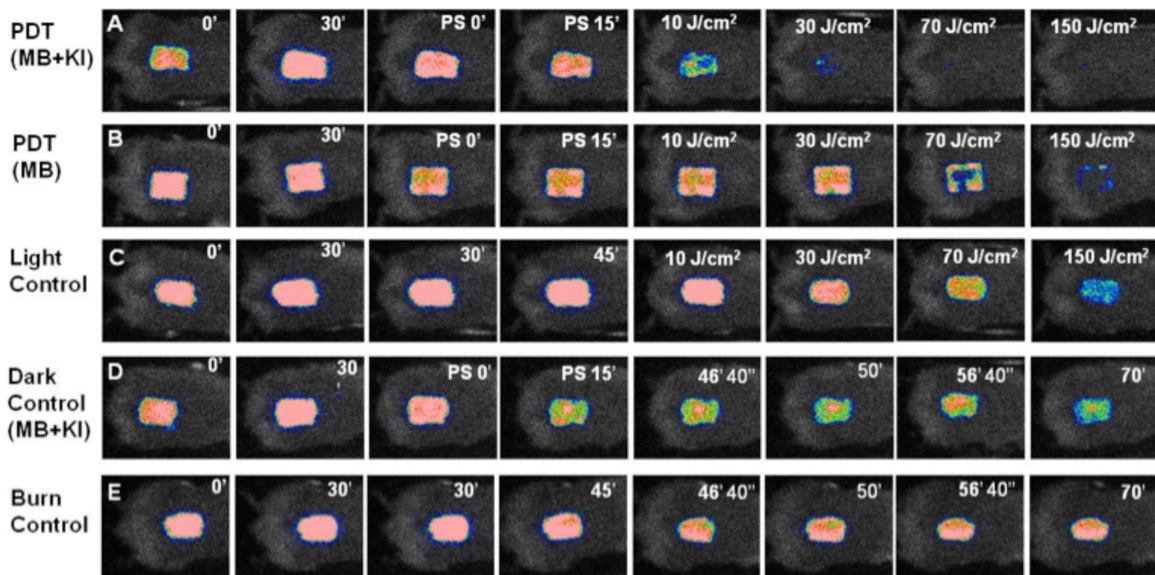


FIG 7 (A to E) Successive bacterial bioluminescence images of representative mouse burns infected with 10^8 CFU of luminescent MRSA (USA300) and treated with PDT using a mixture of MB (50 μ M) and KI (10 mM) (A) or PDT using MB (50 μ M) at 30 min after bacterial inoculation and 15 min from PS application (B). PDT was carried out with a combination of 50 μ l of a mixture containing MB and KI or MB alone and 150 J/cm² red light (660 ± 15 nm; 100 mW/cm²). (C) Light alone. (D) Application of a mixture of MB and KI but without red light illumination (dark control). (E) Burn control without any treatment. (F) Dose response of mean bacterial bioluminescence of mouse burns infected with MRSA (USA300) after treatment with light alone, a mixture of MB (50 μ M) and KI (10 mM) (dark control), PDT using MB (50 μ M) alone, or a mixture of MB (50 μ M) and KI (10 mM).

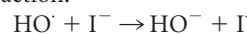
bioluminescence from mouse wounds treated with MB (Fig. 7B) or MB plus KI (Fig. 7A) during PDT treatment. The amount of light required to eradicate bacteria from the wound was much less when the MB plus KI solution was irradiated than when MB alone was irradiated.

In Fig. 7F, we show the dose response curves of all groups. Each curve represents the average \pm standard error of the mean (SEM) of bacterial bioluminescence in each group ($n = 6$). PDT using MB induced a decrease of around 2 log units in bacterial bioluminescence while the MB plus KI solution induced up to 3.5 log unit reductions during the same time.

Figure 8 shows the follow-up monitoring of the bioluminescence images (time courses over 5 days) after PDT in representative mice from all groups. Consistent differences were observed in bacterial regrowth between PDT performed by using MB plus KI (Fig. 8A) and the other groups (Fig. 8B, C, D, and E). In the first

case, the regrowth was minimal. This means that the presence of KI increased the efficacy of PDT at the first treatment to produce sufficient bacterial killing to reduce the recurrence observed during the days postinfection, when MB-PDT alone was not effective to prevent recurrence. The time courses (from day 0 to day 10) of the mean bacterial bioluminescence signal of infected wounds in the different groups of mice are shown in Fig. 8B. The areas under the curve (Fig. 8C) were compared, and PDT with MB plus KI (group E) was significantly lower than all other groups.

In conclusion, on the basis of our results, it seems that the mechanism of the synergistic effect of KI with MB-PDT producing an increase of bacterial killing involves the generation of short-lived reactive iodine species. HO[•] generated in PDT as well as the HO[•] generated in Fenton reaction can produce the following reaction:



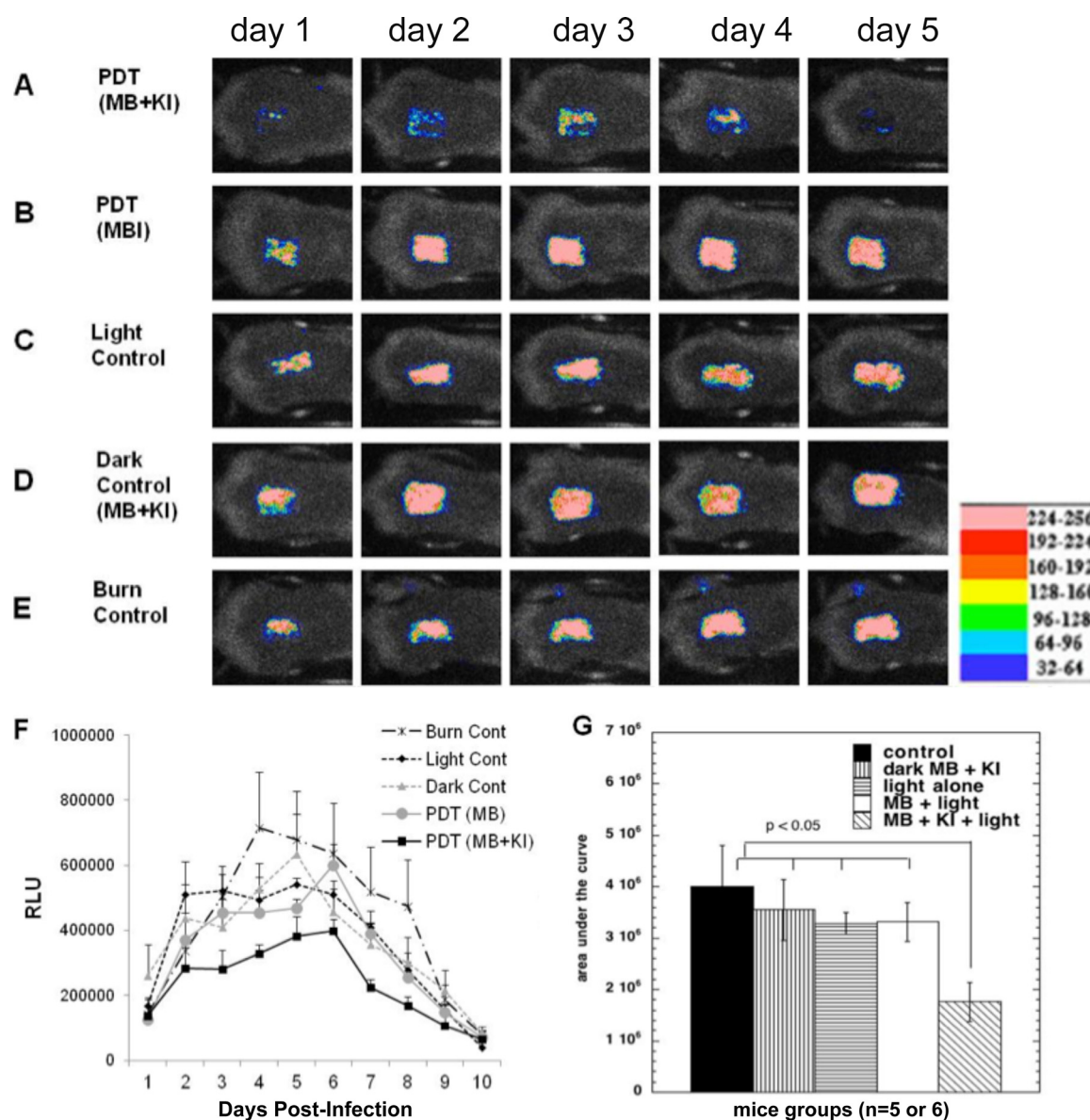
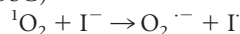
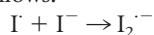


FIG 8 (A to E) Successive bioluminescence images of the follow-up (days 1 to 5 postinfection) of representative mouse burns infected with MRSA (USA300) and treated with PDT using a mixture of MB and KI (A), PDT using MB alone (B), light alone (C), or a mixture of MB and KI but without red light illumination (dark control) (D). (E) Burn control without any treatment. (F) Time courses of quantified mean bacterial bioluminescence values from all the mice in the different groups \pm SEM. (G) Mean areas under the bioluminescence time curves (in the two-dimensional coordinate system determined from panel F) \pm SEM.

Moreover, KI can also react with singlet oxygen (however, this is less likely considering the quenching of HPF activation but not SOSG)



From these reactions, we have generation of I^{\cdot} that is highly unstable and cannot exist itself; it reacts with the iodide anion as follows:



All these species are highly reactive, and we believe these are the major species involved in the enhancement of bacterial killing in the presence of KI using MB-PDT.

The nontoxic nature of KI and its ability to enhance the *in vivo* PDT against infections argue in favor of early clinical testing.

ACKNOWLEDGMENT

This study was supported by the U.S. NIH (grant R01AI050875).

REFERENCES

1. Fair RJ, Tor Y. 2014. Antibiotics and bacterial resistance in the 21st century. *Perspect Medicin Chem* 6:25–64.
2. Hamblin MR, Hasan T. 2004. Photodynamic therapy: a new antimicrobial approach to infectious disease? *Photochem Photobiol Sci* 3:436–450. <http://dx.doi.org/10.1039/b311900a>.
3. Garland MJ, Cassidy CM, Woolfson D, Donnelly RF. 2009. Designing photosensitizers for photodynamic therapy: strategies, challenges and promising developments. *Future Med Chem* 1:667–691. <http://dx.doi.org/10.4155/fmc.09.55>.
4. Huang L, Xuan Y, Koide Y, Zhiyentayev T, Tanaka M, Hamblin MR. 2012. Type I and type II mechanisms of antimicrobial photodynamic ther-

- apy: an *in vitro* study on Gram-negative and Gram-positive bacteria. *Lasers Surg Med* 44:490–499. <http://dx.doi.org/10.1002/lsm.22045>.
5. Wan W, Yeow JT. 2012. Antibacterial properties of poly(quaternary ammonium) modified gold and titanium dioxide nanoparticles. *J Nanosci Nanotechnol* 12:4601–4606. <http://dx.doi.org/10.1166/jnn.2012.6147>.
 6. Marotti J, Sperandio FF, Fregnani ER, Aranha AC, de Freitas PM, Eduardo CDP. 2010. High-intensity laser and photodynamic therapy as a treatment for recurrent herpes labialis. *Photomed Laser Surg* 28:439–444. <http://dx.doi.org/10.1089/pho.2009.2522>.
 7. Sperandio FF, Marotti J, Aranha AC, Eduardo CDP. 2009. Photodynamic therapy for the treatment of recurrent herpes labialis: preliminary results. *Gen Dent* 57:415–419.
 8. de Oliveira BP, Aguiar CM, Camara AC. 2014. Photodynamic therapy in combating the causative microorganisms from endodontic infections. *Eur J Dent* 8:424–430. <http://dx.doi.org/10.4103/1305-7456.137662>.
 9. Klepac-Ceraj V, Patel N, Song X, Holewa C, Patel C, Kent R, Amiji MM, Soukos NS. 2011. Photodynamic effects of methylene blue-loaded polymeric nanoparticles on dental plaque bacteria. *Lasers Surg Med* 43:600–606.
 10. Siddiqui SH, Awan KH, Javed F. 2013. Bactericidal efficacy of photodynamic therapy against *Enterococcus faecalis* in infected root canals: a systematic literature review. *Photodiagnosis Photodyn Ther* 10:632–643. <http://dx.doi.org/10.1016/j.pdpdt.2013.07.006>.
 11. Huang L, St Denis TG, Xuan Y, Huang YY, Tanaka M, Zadlo A, Sarna T, Hamblin MR. 2012. Paradoxical potentiation of methylene blue-mediated antimicrobial photodynamic inactivation by sodium azide: role of ambient oxygen and azide radicals. *Free Radic Biol Med* 53:2062–2071. <http://dx.doi.org/10.1016/j.freeradbiomed.2012.09.006>.
 12. St Denis TG, Vecchio D, Zadlo A, Rineh A, Sadasivam M, Avci P, Huang L, Kozinska A, Chandran R, Sarna T, Hamblin MR. 2013. Thiocyanate potentiates antimicrobial photodynamic therapy: *in situ* generation of the sulfur trioxide radical anion by singlet oxygen. *Free Radic Biol Med* 65:800–810. <http://dx.doi.org/10.1016/j.freeradbiomed.2013.08.162>.
 13. Food and Drug Administration. 2001. Guidance on potassium iodide as a thyroid blocking agent in radiation emergencies. Food and Drug Administration, Washington, DC.
 14. Hassan I, Keen A. 2012. Potassium iodide in dermatology. *Indian J Dermatol Venereol Leprol* 78:390–393. <http://dx.doi.org/10.4103/0378-6323.95472>.
 15. Sterling JB, Heymann WR. 2000. Potassium iodide in dermatology: a 19th century drug for the 21st century—uses, pharmacology, adverse effects, and contraindications. *J Am Acad Dermatol* 43:691–697. <http://dx.doi.org/10.1067/mjd.2000.107247>.
 16. Costa RO, Macedo PM, Carvalhal A, Bernardes-Engemann AR. 2013. Use of potassium iodide in dermatology: updates on an old drug. *An Bras Dermatol* 88:396–402. <http://dx.doi.org/10.1590/abd1806-4841.20132377>.
 17. Dai T, Gupta A, Huang YY, Sherwood ME, Murray CK, Vrahas MS, Kielian T, Hamblin MR. 2013. Blue light eliminates community-acquired methicillin-resistant *Staphylococcus aureus* in infected mouse skin abrasions. *Photomed Laser Surg* 31:531–538. <http://dx.doi.org/10.1089/pho.2012.3365>.
 18. Miyachi Y, Niwa Y. 1982. Effects of potassium iodide, colchicine and dapsone on the generation of polymorphonuclear leukocyte-derived oxygen intermediates. *Br J Dermatol* 107:209–214. <http://dx.doi.org/10.1111/j.1365-2133.1982.tb00340.x>.
 19. Gebicki JM, Guille J. 1989. Spectrophotometric and high-performance chromatographic assays of hydroperoxides by the iodometric technique. *Anal Biochem* 176:360–364. [http://dx.doi.org/10.1016/0003-2697\(89\)90323-0](http://dx.doi.org/10.1016/0003-2697(89)90323-0).
 20. Klebanoff SJ. 1982. The iron-H₂O₂-iodide cytotoxic system. *J Exp Med* 156:1262–1267. <http://dx.doi.org/10.1084/jem.156.4.1262>.
 21. Levitz SM, Diamond RD. 1984. Killing of *Aspergillus fumigatus* spores and *Candida albicans* yeast phase by the iron-hydrogen peroxide-iodide cytotoxic system: comparison with the myeloperoxidase-hydrogen peroxide-halide system. *Infect Immun* 43:1100–1102.
 22. Sugar AM, Chahal RS, Brummer E, Stevens DA. 1984. The iron-hydrogen peroxide-iodide system is fungicidal: activity against the yeast phase of *Blastomyces dermatitidis*. *J Leukoc Biol* 36:545–548.
 23. Klebanoff SJ. 1967. Iodination of bacteria: a bactericidal mechanism. *J Exp Med* 126:1063–1078. <http://dx.doi.org/10.1084/jem.126.6.1063>.
 24. Ihalin R, Nuutila J, Loimaranta V, Lenander M, Tenovuo J, Lilius EM. 2003. Susceptibility of *Fusobacterium nucleatum* to killing by peroxidase-iodide-hydrogen peroxide combination in buffer solution and in human whole saliva. *Anaerobe* 9:23–30. [http://dx.doi.org/10.1016/S1075-9964\(03\)00005-2](http://dx.doi.org/10.1016/S1075-9964(03)00005-2).
 25. Kohler H, Jenzer H. 1989. Interaction of lactoperoxidase with hydrogen peroxide. Formation of enzyme intermediates and generation of free radicals. *Free Radic Biol Med* 6:323–339.
 26. Chance B. 1999. The kinetics of the enzyme-substrate compound of peroxidase. 1943. *Adv Enzymol Relat Areas Mol Biol* 73:3–23.
 27. Vanden Abbeele A, De Meel H, Courtois P, Pourtois M. 1996. Influence of a hypoiodite mouth-wash on dental plaque formation *in vivo*. *Bull Group Int Rech Sci Stomatol Odontol* 39:57–61.
 28. Bosch EH, van Doorne H, de Vries S. 2000. The lactoperoxidase system: the influence of iodide and the chemical and antimicrobial stability over the period of about 18 months. *J Appl Microbiol* 89:215–224. <http://dx.doi.org/10.1046/j.1365-2672.2000.01098.x>.